Time-Reversal-Breaking Weyl Fermions in Magnetic Heusler Alloys

Zhijun Wang, M. G. Vergniory, S. Kushwaha, Max Hirschberger, E. V. Chulkov, A. Ernst, N. P. Ong, Robert J. Cava, and B. Andrei Bernevig

Time-Reversal Breaking Weyl Fermions In Magnetic Heuslers

Zhijun Wang[1], M. G. Vergniory[2,3],*, S. Kushwaha[4], Max Hirschberger[1], E. V. Chulkov[2,5,7], A. Ernst[6], N. P. Ong[1], Robert J. Cava[4], and B. Andrei Bernevig[1]

[1]*Department of Physics, Princeton University, Princeton, NJ 08544, USA*
[2]*Donostia International Physics Center, P. Manuel de Lardizabal 4, 20018 Donostia-San Sebastián, Spain*
[3] *Department of Applied Physics II, Faculty of Science and Technology,*
University of the Basque Country UPV/EHU, Apdo. 644, 48080 Bilbao, Spain
[4]*Department of Chemistry, Princeton University, Princeton, NJ 08540, USA*
[5] *Departamento de Física de Materiales, Universidad del País Vasco/Euskal*
Herriko Unibertsitatea UPV/EHU, 20080 Donostia-San Sebastián, Spain
[6] *Max-Planck-Institut für Mikrostrukturphysik, Weinberg 2, D-06120 Halle, Germany and*
[7] *Saint Petersburg State University, 198504 Saint Petersburg, Russia*

Weyl fermions have recently been observed in several time-reversal invariant semimetals and photonics materials with broken inversion symmetry. These systems are expected to have exotic transport properties such as the chiral anomaly. However, most discovered Weyl materials possess a substantial number of Weyl nodes close to the Fermi level that give rise to complicated transport properties. Here we predict for the first time a new family of Weyl systems defined by broken time reversal symmetry, namely, Co-based magnetic Heusler materials XCo_2Z (X = IVB or VB; Z = IVA or IIIA). To search Weyls in the centrosymmetric magnetic systems, we recall an easy and practical inversion invariant, which has been calculated to be -1, guaranteeing the existence of an odd number of pairs of Weyls. These materials exhibit, when alloyed, only two Weyl nodes at the Fermi level - the minimum number possible in a condensed matter system. The Weyl nodes are protected by the rotational symmetry along the magnetic axis and separated by a large distance (of order 2π) in the Brillouin zone. The corresponding Fermi arcs have been calculated as well. This discovery provides a realistic and promising platform for manipulating and studying the magnetic Weyl physics in experiments.

Weyl fermions are theorized to exist in the standard model above the symmetry breaking scale - at low-energy scales they invariably acquire mass. As such, the search for Weyl fermions has shifted to condensed matter systems, where they appear as unremovable crossings in electronic Bloch bands, close to the Fermi level, in 3-spatial dimensions. They recently became a reality with the experimental discovery [1, 2] of the theoretically predicted [3, 4] Weyl semimetals (WSM) in the TaAs family of compounds. Topological Weyl metals are responsible for an array of exotic spectroscopic and transport phenomena such as the surface disconnected Fermi arcs, chiral anomaly and anomalous Hall effects [5–12].

Transport in Weyl materials reveal the fundamental nature of the Berry phase in magneto transport. The chiral anomaly is reflected in the negative longitudinal magnetoresistance (NMR), which on its own stems from the Weyl fermions. A minumum number (2) of Weyls could make it easier to observe the NMR than for cases with a large number of Weyls. Due to the fermion doubling problem, Weyl nodes appear in multiples of 2. With time-reversal invariance, this number raises to multiples of 4. The TaAs family of compounds exhibits 24 Weyl nodes, due to several other mirror symmetries. This large number of Weyls gives rise to complicated spectroscopic and transport properties. By comparison, the hypothetical hydrogen atom of Weyl semimetals is a material with only 2 Weyl nodes at the Fermi level (E_F), preferably cleanly separated in momentum space and in energy from other bands.

In previous work [13], $HgCr_2Se_4$ has been predicted to be a Chern (*not* Weyl) semimetal with two crossing points, each of which possesses chirality of 2. Also, the existence of only two Weyl nodes is also expected in the Topological/normal-insulator heterostructures with magnetic doping [14, 15]. Unfortunately, none of these systems have been verified so far. In this paper we predict for the first time a series of magnetic Heusler compounds that can exhibit, when alloyed, two Weyl points close to Fermi energy and largely separated in momentum space. Magnetic Heusler compounds have several advantages over the other compounds where Weyl fermions have been proposed and detected. First they are ferromagnetic half-metallic compounds with Curie temperatures up to the room temperature [16], meaning they can be of great use for spin manipulation and spintronics applications. Second, they exhibit Weyl fermions, with the large associated Berry phase of their Fermi surfaces. As such, the anomalous Hall effect and spin Hall effect in these materials is theoretically expected to be large, which has already been confirmed in initial experimental studies [17–19]. Third, the magnetism in these materials is "soft", meaning that an applied magnetic field can easily change the magnetic moment direction: a similar phenomenon has been observed in GdPtBi [20, 21]. Since, as pointed out in the Supplementary Material [22, 43], the structure and direction of Weyls depends on the magnetic field, the magnetic Heuslers provide us a realistic
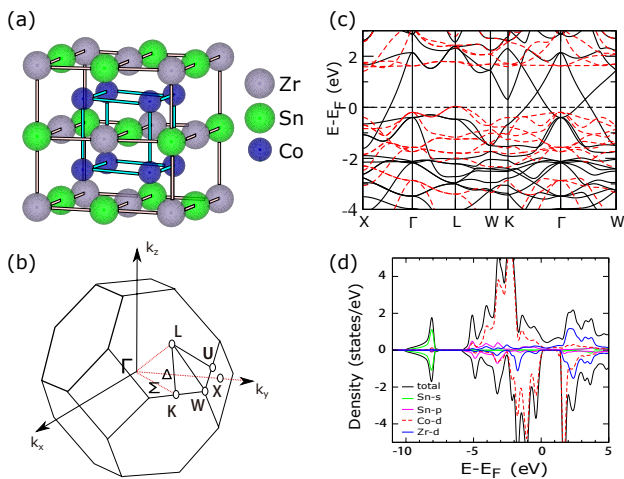
FIG. 1. (a) Rocksalt crystal structure of ZrCo$_2$Sn with $Fm\bar{3}m$ space group. Co, Zr and Sn atoms are shown in blue, gray and green, respectively. (b) Brillouin zone (BZ) of the rocksalt structure. It has three independent time-reversal-invariant points, $\Gamma(0,0,0)$, $L(\frac{\pi}{a},\frac{\pi}{a},\frac{\pi}{a})$, and $X(\frac{2\pi}{a},0,0)$. (c) Bulk band structure of ZrCo$_2$Sn along high symmetry lines without spin-orbit coupling (SOC). The majority and minority spin bands are indicated by solid-black and dashed-red lines, respectively. (d) Total and partial density of states without SOC, the positive (negative) lines represent the majority (minority) spin channel.

and promising platform for manipulating and studying the magnetic Weyl physics in experiments.

Based on the first principle calculations with the magnetism oriented in the [110] direction, we found two Weyl nodes, related by symmetry, appear on the same axis. Their energy relative to the Fermi level can be tuned by alloying, and we provide an estimation of the appropriate concentration of the dopant necessary to tune the Weyls to the Fermi level. We carry out a symmetry analysis and solidify our ab-initio claims of the existence of Weyl nodes by showing that they are formed by bands of opposite C_2 eigenvalues. Furthermore we link the existence of Weyl nodes to the existence of an inversion invariant discovered earlier[44] in the theory of inversion symmetric topological insulators. We then obtain the structure of the Fermi arcs on 001-surface. We expand upon the results in the Supplementary Material, where we also analyze the possible topological scenarios under different potential magnetization directions, and present magnetization data on one of the synthesized materials from our proposals.

Our proposed candidates for Weyl metals are the Co-based Heusler compounds: XCo$_2$Z (X = IVB or VB; Z = IVA or IIIA) with $N_v = 26$, denoting the number of valence electrons (s, d electrons for the transition metals and s, p electrons for the main group element). This family of Co-based Heusler compounds follows the Slater-Pauling rule which predicts a total spin magnetic moment

$m = N_v - 24$ (the number of atoms $\times$ 6) [45–47]. In this paper we focus on a representative candidate - ZrCo$_2$Sn that we have synthesized experimentally [16]. We present the results for the rest of the compounds in the Supplementary Material. We show that the interesting Weyl nodes of all the 26-electron compounds are about 0.6 eV above the Fermi energy. However, there is another Co-based Heusler family with 27-electron, that are also candidates for Weyl metals and have been synthesized experimentally [16], such as NbCo$_2$Sn and VCo$_2$Sn, making it possible to move the Weyl nodes close to or at the Fermi level by alloying. The Co-based Heusler compounds, with their great diversity, give us the opportunity to tune our compounds (e.g. the number of valence electrons, spin-orbit coupling strength, etc.) across different compositions in order to get the desired properties.

We perform ab-initio calculations based on the density functional theory (DFT) [48, 49] and the generalized gradient approximation (GGA) for the exchange-correlation potential [50] (more details in Supplementary Material). The spin-polarized band structure and density of states (DOS) of ZrCo$_2$Sn are calculated within GGA+U without SOC, shown in Fig. 1(c) and Fig. 1(d) respectively. The value of U was chosen to be 3 eV, which provides Curie temperature close to the experimental value [51] and reproduces the measured magnetic moment (see Fig. 5 of Supplementary Material section). The Curie temperature was computed by means of Random-Phase Approximation by S. V. Tyablikov [52]. We have tested U with different functionals, such as LDA [53], PBE [50] and PBEsol [54], and get the same result (detailed calculation of U as a fucntion of T_C and the magnetic coupling constants can be found in the Supplementary Material section). In the following we will use the PBE pseudopotential.

In Fig. 1(c), we see a band gap in the minority states around E_F, which has been double-checked with the modified Becke-Johnson exchange potential [55]. This suggests a good half-metallic property, which is consistent with the experimental investigation of the spin-resolved unoccupied density of states of the partner compound TiCo$_2$Sn [56]. The calculated partial DOS, shown in Fig. 1(d), suggests the states of ZrCo$_2$Sn around E_F are mostly of d character, namely Co-d and Zr-d states. After including SOC, the calculated band structure in Fig. 2(c) shows the SOC has little influence on the electronic structure and the half-metallic ferromagnetism, because the SOC strengths of both Co and Zr are small. We performed ab-initio calculations to determine the energetically most favorable magnetization direction - the [110] easy axis. However, this magnetic configuration is energetically very close to the [100]. we assume the magnetism is along the [110] axis in the main text. The analysis of the [100] magnetism is presented in Supplementary Material, which also shows topological properties such as Weyl points and nodal lines in the band structure.
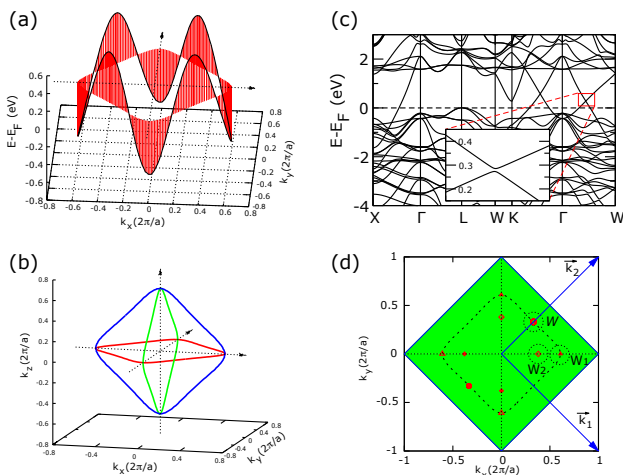
FIG. 2. (a) Nodal line in the xy plane has a big dispersion. (b) Three nodal lines in three planes in three-dimensional (3D) k-space. (c) The SOC band sturcture of $ZrCo_2Sn$ with the [110] magnetism, opening a small gap in the ΓW direction in the inset. (d) Weyl points emerge with SOC. The independent W, W_1 and W_2 points are clearly indicated in the figure (top view) - the remaining ones can be obtained by symmetry. W and W_1 is in the xy plane, while the W_2 is out of the plane. The Chern numbers can be calculated with the Wilson-loop method applied on a sphere (illustrated as dashed circles) enclosing a Weyl point. The filled (unfilled) symbols indicate Chern number $+1$ (-1). Furthermore, the 001-surface lattice vectors are also given as $\vec{k}_1(\frac{2\pi}{a}, -\frac{2\pi}{a})$ and $\vec{k}_2(\frac{2\pi}{a}, \frac{2\pi}{a})$, and the corresponding surface BZ is painted in green.

In the spin-polarized calculation, neglecting SOC, the spin and the orbitals are independent and regarded as different subspaces. In that sense, the spatial crystal symmetries of O_h^5 have no effect on the spin degree of freedom, and the two spin channels are decoupled. Once SOC is considered, the two spin channels couple together, and symmetries can decrease depending on the direction of the spontaneous magnetization. For instance, the mirror reflection M_z is a symmetry without SOC included. With SOC it is broken as the magnetization is along [110]. However, the product between time-reversal and reflection symmetries (TM_z) is still a magnetic symmetry, even though SOC is included. The corresponding magnetic space group of [110] spin-polarization contains only 8 elements formed by three generators: inversion $\mathcal{I}$, 2-fold rotation $C2_{110}$ around 110 axis and the product ($TC2_z$) of time-reversal and rotation $C2_z$, which allows for the existence of Weyl points (WPs) in the xy-plane [57].

We first elucidate the band topology in the absence of SOC. From the spin-polarized band structure in Fig. 1(c), we can observe that two bands crossings occur along ΓX, ΓW and ΓK in the majority spin. Actually, these crossings are in the xy-plane, which respects the mirror sym-

metry M_z. Bands within this plane can be classified by mirror eigenvalues ± 1. Further symmetry analysis shows that the two bands belong to opposite mirror eigenvalues, giving rise to a nodal line in the xy plane [3, 58]. The energy of the nodal line disperses dramatically in the xy plane, as shown in Fig. 2(a). The minimum of this dispersion is in the ΓX (or [100]) direction and the maximum is in the ΓK (or [110]) direction. In addition to the nodal line in the xy-plane, two similar nodal lines are also found in the xz-plane and yz-plane related by a $C4$ rotation around the x, y coordinate axis. As a result, the three nodal lines in different planes intersect at six different points as depicted in Fig. 2(b).

Once introducing SOC, with a magnetization along the [110] direction, the mirror symmetries M_z, M_x and M_y are all broken. In the absence of other symmetries, these nodal lines in the mirror planes would become fully gapped. However, along the magnetization [110] direction, a pair of Weyl points survive, protected by the $C2_{110}$ rotation. Namely, the crossing bands belong to different $C2_{110}$ eigenvalues $\pm i$ on the high-symmetry line. The coordinates of these WPs (W), related by inversion $\mathcal{I}$, are given in Tab. I. Their location and Chern numbers are illustrated in Fig.2(d). An inversion eigenvalue argument shows us that we must have $4k + 2$, $k \in \mathcal{Z}$, number of Weyls in this system (see Supplementary Material): the product of the inversion eigenvalues of the occupied bands at the inversion symmetric points is -1, signaling the presence of an odd number of pairs of Weyls [44].

In addition, deriving from the nodal line in the xy-plane, other four Weyls are found slightly away from the coordinate axis in the plane. The presence of Weyls in a high symmetry plane is allowed by the antiunitary symmetry $TC2_z$ [57]. The quadruplet Weyls (W_1) are related to each other by $\mathcal{I}$ and $C2_{110}$. Their precise positions and topological charges are presented in Tab. I. After carefully checking other two nodal lines, we see that a third kind of Weyl points (W_2), different from the previous two kinds, does not prefer any special direction, but distributes near the xz- and yz-plane. As these Weyls are generic points without any little-group symmetry, the octuplet Weyls W_2 are related by all the three generators of the magnetic group. As a result, the position of the W_2 changes considerably from $TiCo_2Sn$, to $ZrCo_2Sn$ to $HfCo_2Sn$, following the nodal lines without SOC. In principle, this kind of Weyls are not stable (in contrast, the W-Weyls are stablized by the $C2_{110}$ symmetry on the [110] axis), as they can be moved close in the z-axis and thereby annihilate with each other. The average charge centers obtained by the Wilson-loop method on the spheres (W, W_1 and W_2) are presented in Fig. 3(a). All the Chern numbers of the three Weyls are shown in Table I, and their positions are shown in Fig. 2(d). As the energy level of W_1 is very low and W_2 could be removed by tuning SOC, we will focus on the doublet Weyls W.

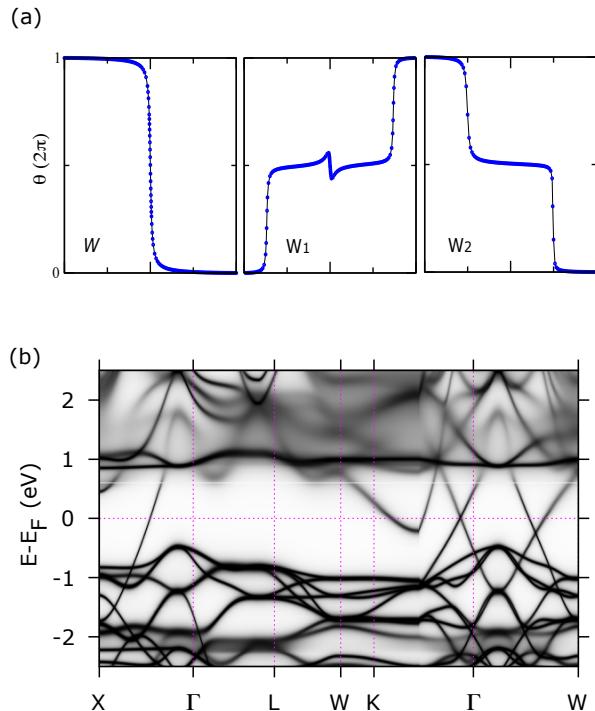We now focus on the two W type Weyls (located at 0.6

(a)

(b)

FIG. 3. (a) The flow chart of the average position of Wannier centers obtained by the Wilson-loop method applied on a sphere that encloses a node [57]. The average center shifts downwards, corresponding to Chern mumber -1 for W and W_2, while it shifts upwards, suggesting the Chern mumber of W_1 is $+1$. (b) Calculated Bloch spectral function of $Zr_{0.725}Nb_{0.275}Co_2Sn$ along high symmetry lines.

TABLE I. WPs of $ZrCo_2Sn$. The Weyl nodes' positions (in reduced coordinates k_x, k_y, k_z), Chern numbers, and the energy relative to the E_F of the unalloyed compound. The WPs in $ZrCo_2Sn$ are formed by two bands which in the absence of SOC would form nodal lines. W and W_1, are stable in the xy plane, while the W_2 stable out of the plane. The coordinates of the other Weyl points are related to the ones listed by the symmetries, $\mathcal{I}$, $C2_{110}$ and $\mathcal{T}C2_z$.

Weyl points	coordinates	Chern number	$E - E_F$
	$(k_x \frac{2\pi}{a}, k_y \frac{2\pi}{a}, k_z \frac{2\pi}{a})$		(eV)
W	$(0.334, 0.334, 0)$	-1	$+0.6$
W_1	$(0.58, -0.0005, 0)$	$+1$	-0.6
W_2	$(0.40, 0.001, \pm0.28)$	-1	$+0.3$

eV over the Fermi level in the K−Γ (or [110]) direction. Our goal now is to tune the energy of the WP to the Fermi level. For this purpose we consider other compounds with the same stoichiometry, more electrons and similar lattice parameter. As we mentioned before, $NbCo_2Sn$, which have the same crystal structure [16], contains one more electron per a unit cell than that of $ZrCo_2Sn$. Therefore, one can expect that alloying $ZrCo_2Sn$ with Nb in
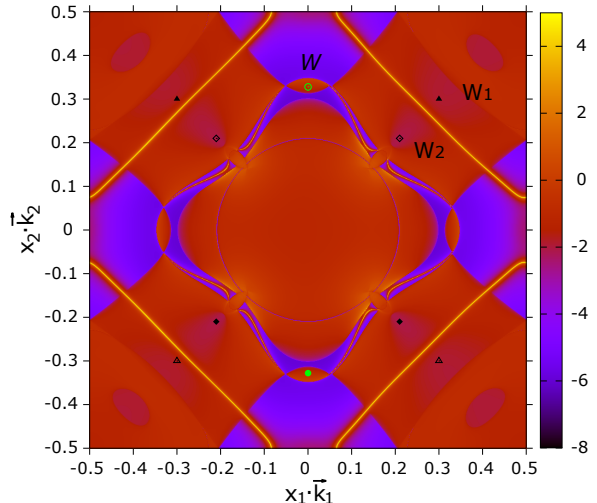

FIG. 4. Bloch spectral function of the (001)-surface at 0.5 eV above the Fermi level for $ZrCo_2Sn$. In the (001)-surface Brillouin zone, the surface **k**-points are represented by $x_1\vec{k}_1 + x_2\vec{k}_2$. The surface lattice vectors ($\vec{k}_1$ and $\vec{k}_2$) are illustrated, and the corresponding surface BZ is shown as green-colored area in Fig. 2(d) (notice the $\pi/2$ rotation of the surface BZ). Only the bulk projections of W (yellow-colored) are separated from the Fermi surfaces projections. The bulk projections of W_1 and W_2 (black-colored) sit inside the projection of the bulk Fermi surfaces. The Fermi arcs connecting to the bulk projections of W are shown. The large, square surface states is of a trivial nature. The color code represents $log(\rho)$.

the Zr site would shift down the WP energy while keeping the main band topology unchanged. Using a first-principles Green's function method, we dope $ZrCo_2Sn$ with Nb. Disorder effects were taken into account within a coherent potential approximation (CPA) [59]. Varying Nb content, we search for a concentration, which brings the W Weyls to the Fermi level. Fig. 3(b) shows the calculated spectral function for $Zr_{1-x}Nb_xCo_2Sn$ (with $x = 0.275$). By inversion ($\mathcal{I}$) symmetry, there exist another Weyl point separated in k-space by $\sim 2\pi$ with the same energy. In the same line, the experimental existence of VCo_2Sn [16] also motivate us to dope the partner compound $Ti_{1-x}V_xCo_2Sn$ as well, and our calculations suggest $x = 0.1$.

Given that the Weyl nodes W, W_1 and W_2 all resulted from the connected nodal lines in the absence of SOC, a large residual Fermi surface has a projection on any surface of the material. Hence the Fermi arcs emanating from the W Weyl points are interrupted by the residual projection of bulk Fermi surfaces on the surface of the material. However, the Fermi arc signatures of W-Weyls are still clear as can be seen in Fig. 4 where we plot the surface spectral function for the (001)-surface of $ZrCo_2Sn$. Since the bulk Fermi surface projections

where W_1 and W_2 are located overlap, the Fermi arcs connections are not guaranteed at some certain energies. Furthermore, a trivial square surface state is found as well, due to the hanging bonding at the surface.

In conclusion we have predicted theoretically that a new family of Co-based magnetic Heuslers realize Weyl systems with several Weyl nodes whose position in energy can be tuned by alloying. We have performed ab-initio calculations of a representative ferromagnetic compound $ZrCo_2Sn$. For the [110] magnetization we find two Weyl points related by $\mathcal{I}$ symmetry situated on the same axis. By means of a first-principles Green's function method, we doped the $ZrCo_2Sn$ with Nb and showed that these two Weyls can be shifted to the Fermi level. Finally, we obtained the Fermi arc structure of this class of materials. This discovery shows a way to the realizing the hydrogen atom of Weyl materials and provides a promising platform for studying exotic properties of magnetic Weyls in experiments.

---

* Zhijun Wang and M. G. Vergniory contributed equally to this work

[1] B. Q. Lv, H. M. Weng, B. B. Fu, X. P. Wang, H. Miao, J. Ma, P. Richard, X. C. Huang, L. X. Zhao, G. F. Chen, Z. Fang, X. Dai, T. Qian, and H. Ding, Phys. Rev. X **5**, 031013 (2015).

[2] S.-Y. Xu, I. Belopolski, N. Alidoust, M. Neupane, G. Bian, C. Zhang, R. Sankar, G. Chang, Z. Yuan, C.-C. Lee, S.-M. Huang, H. Zheng, J. Ma, D. S. Sanchez, B. Wang, A. Bansil, F. Chou, P. P. Shibayev, H. Lin, S. Jia, and M. Z. Hasan, Science **349**, 613 (2015).

[3] H. Weng, C. Fang, Z. Fang, B. A. Bernevig, and X. Dai, Phys. Rev. X **5**, 011029 (2015).

[4] S.-M. Huang, S.-Y. Xu, I. Belopolski, C.-C. Lee, G. Chang, B. Wang, N. Alidoust, G. Bian, M. Neupane, C. Zhang, S. Jia, A. Bansil, H. Lin, and M. Z. Hasan, Nat. Commun. (2015), doi:10.1038/ncomms8373.

[5] H. Nielsen and M. Ninomiya, Physics Letters B **130**, 389 (1983).

[6] X. Wan, A. M. Turner, A. Vishwanath, and S. Y. Savrasov, Phys. Rev. B **83**, 205101 (2011).

[7] J. Xiong, S. K. Kushwaha, T. Liang, J. W. Krizan, M. Hirschberger, W. Wang, R. J. Cava, and N. P. Ong, Science **350**, 413 (2015).

[8] X. Huang, L. Zhao, Y. Long, P. Wang, D. Chen, Z. Yang, H. Liang, M. Xue, H. Weng, Z. Fang, X. Dai, and G. Chen, Phys. Rev. X **5**, 031023 (2015).

[9] J. Liu and D. Vanderbilt, Phys. Rev. B **90**, 155316 (2014).

[10] M. Hirayama, R. Okugawa, S. Ishibashi, S. Murakami, and T. Miyake, Phys. Rev. Lett. **114**, 206401 (2015).

[11] T. c. v. Bzdušek, A. Rüegg, and M. Sigrist, Phys. Rev. B **91**, 165105 (2015).

[12] A. A. Burkov, Phys. Rev. Lett. **113**, 187202 (2014).

[13] G. Xu, H. Weng, Z. Wang, X. Dai, and Z. Fang, Phys. Rev. Lett. **107**, 186806 (2011).

[14] A. A. Burkov and L. Balents, Phys. Rev. Lett. **107**, 127205 (2011).

[15] D. Bulmash, C.-X. Liu, and X.-L. Qi, Phys. Rev. B **89**, 081106 (2014).

[16] A. Carbonari, R. Saxena, W. Pendl, J. M. Filho, R. Attili, M. Olzon-Dionysio, and S. de Souza, Journal of Magnetism and Magnetic Materials **163**, 313 (1996).

[17] S. Wurmehl, G. H. Fecher, H. C. Kandpal, V. Ksenofontov, C. Felser, H.-J. Lin, and J. Morais, Phys. Rev. B **72**, 184434 (2005).

[18] T. Graf, J. Winterlik, L. Muchler, G. H. Fecher, C. Felser, and S. S. Parkin, Handbook of Magnetic Materials, **21**, 1 (2013).

[19] W. Zhang, Z. Qian, Y. Sui, Y. Liu, W. Su, M. Zhang, Z. Liu, G. Liu, and G. Wu, Journal of Magnetism and Magnetic Materials **299**, 255 (2006).

[20] C. S. *et al.*, arXiv:1604.01641.

[21] M. H. *et al.*, Nat. Mat. (2016), doi:10.1038/nmat4684.

[22] See Supplemental Material [url], which includes Refs. [23-42], for the details on the band structures of other candidates, detailed calculation methods, experimental measurements, inversion symmetry characterization and symmetry analysis. The results of 100-magnetism are presented as well.

[23] E. Goerlich, R. Kmiec, K. Latka, T. Matlak, K. Ruebenbauer, A. Szytula, and K. Tomala, Physica Status Solidi A: Applied Research **30**, 765 (1975).

[24] E. Goerlich, K. Latka, D. Szytula, A.and Wagner, R. Kmiec, and K. Ruebenbauer, Solid State Communications **25**, 661 (1978).

[25] P. Webster and K. Ziebeck, Journal of Physics and Chemistry of Solids **34**, 1647 (1973).

[26] K. Buschow, P. Van Engen, and R. Jongebreur, Journal of Magnetism and Magnetic Materials **8**, 1 (1983).

[27] K. Buschow and P. Van Engen, Journal of Magnetism and Magnetic Materials **25**, 90 (1981).

[28] G. Kresse and J. Furthmueller, Computational Materials Science **6**, 15 (1996).

[29] G. Kresse and J. Hafner, Phys. Rev. B **48**, 13115 (1993).

[30] G. Kresse and D. Joubert, Phys. Rev. B **59**, 1758 (1999).

[31] D. Hobbs, G. Kresse, and J. Hafner, Phys. Rev. B **62**, 11556 (2000).

[32] S. L. Dudarev, G. A. Botton, S. Y. Savrasov, C. J. Humphreys, and A. P. Sutton, Phys. Rev. B **57**, 1505 (1998).

[33] P. G. van Engen, K. H. J. Buschow, and M. Erman, Journal of Magnetism and Magnetic Materials **30**, 374 (1983).

[34] J. Korringa, Physica **13**, 392 (1947).

[35] W. Kohn and N. Rostoker, Phys. Rev. **94**, 1111 (1954).

[36] M. Lueders, A. Ernst, W. M. Temmerman, Z. Szotek, and P. J. Durham, Journal of Physics: Condensed Matter **13**, 8587 (2001).

[37] A. I. Liechtenstein, M. I. Katsnelson, and V. A. Gubanov, Journal of Physics F: Metal Physics **14**, L125 (1984).

[38] R. V. Skolozdra, Y. V. Stadnyk, Y. K. Gorelenko, and E. E. Treletskaya, Sov. Phys. Solid State **32**, 1536 (1990).

[39] K. Momma and F. Izumi, Journal of Applied Crystallography **44**, 1272 (2011).

[40] T. Williams, C. Kelley, and many others, "Gnuplot 4.4: an interactive plotting program," http://gnuplot.sourceforge.net/ (2010).

[41] F. Munoz and A. Romero, "Pyprocar," (2014).

[42] P. Ramachandran and G. Varoquaux, Computing in Science & Engineering **13**, 40 (2011).

[43] S. Chadov, G. H. Fecher, and C. Felser, private communication.

[44] T. L. Hughes, E. Prodan, and B. A. Bernevig, Phys. Rev. B **83**, 245132 (2011).

[45] S. Skaftouros, K. Özdoğan, E. Şaşıoğlu, and I. Galanakis, Phys. Rev. B **87**, 024420 (2013).

[46] I. Galanakis, P. H. Dederichs, and N. Papanikolaou, Phys. Rev. B **66**, 174429 (2002).

[47] G. H. Fecher, H. C. Kandpal, S. Wurmehl, C. Felser, and G. Schoenhense, Journal of Applied Physics **99**, 08J106 (2006).

[48] P. Hohenberg and W. Kohn, Phys. Rev. **136**, B864 (1964).

[49] W. Kohn and L. J. Sham, Phys. Rev. **140**, A1133 (1965).

[50] J. P. Perdew, K. Burke, and M. Ernzerhof, Phys. Rev. Lett. **77**, 3865 (1996).

[51] E. Uchida, N. Fukuoka, H. Kondoh, T. Takeda, Y. Nakazumi, and T. Nagamiya, Journal of the Physical Society of Japan **19**, 2088 (1964), http://dx.doi.org/10.1143/JPSJ.19.2088.

[52] S. V. Tyablikov, *Methods in the Quantum Theory of Magnetism* (Springer Science, 1967).

[53] J. P. Perdew and A. Zunger, Phys. Rev. B **23**, 5048 (1981).

[54] J. P. Perdew, K. Burke, and M. Ernzerhof, Phys. Rev. Lett. **80**, 891 (1998).

[55] F. Tran and P. Blaha, Phys. Rev. Lett. **102**, 226401 (2009).

[56] P. Klaer, M. Kallmayer, C. G. F. Blum, T. Graf, J. Barth, B. Balke, G. H. Fecher, C. Felser, and H. J. Elmers, Phys. Rev. B **80**, 144405 (2009).

[57] A. A. Soluyanov, D. Gresch, Z. Wang, Q. Wu, M. Troyer, X. Dai, and B. A. Bernevig, Nature **527**, 495 (2015).

[58] G. Bian, T.-R. Chang, R. Sankar, S.-Y. Xu, H. Zheng, T. Neupert, C.-K. Chiu, S.-M. Huang, G. Chang, I. Belopolski, D. S. Sanchez, M. Neupane, N. Alidoust, C. Liu, B. Wang, C.-C. Lee, H.-T. Jeng, C. Zhang, Z. Yuan, S. Jia, A. Bansil, F. Chou, H. Lin, and M. Z. Hasan, Nat. Commun. (2016), 10.1038/ncomms10556.

[59] B. L. Gyorffy, Phys. Rev. B **5**, 2382 (1972).